Materials Science & Technology 2006, Symposium on Processing for Reliability
Cincinnati, Ohio, October 15-19, 2006
Edited by William M. Mullins
TMS (The Minerals, Metals & Materials Society), 2006

CONTROLLING SOLIDIFICATION OF PARTICLE LADEN MELTS USING THERMO-MAGNETOHYDRODYNAMICS AND OPTIMIZATION

Marcelo J. Colaço[1], George S. Dulikravich[2]

[1] *Department of Mechanical and Materials Engineering*
Military Institute of Engineering – IME, Rio de Janeiro, RJ 22290-270, Brazil

[2] *Department of Mechanical and Materials Engineering*
Florida International University, 10555 W. Flagler St., Miami, FL 33174, USA

Keywords: solidification, optimization, magnetohydrodynamics, solute transport, smart manufacturing

Abstract

The problem consists of a solidifying thermosolutal flow in a square cavity subjected to variable thermal and magnetic boundary conditions where the objective is to reduce fluid flow intensity by minimizing vertical gradients of solute concentration within the liquid region. A multilevel optimizer based on several deterministic and evolutionary techniques with automatic switching among them, was used together with a response surface formulation in order to optimize thermal and magnetic boundary conditions that will minimize vertical gradients of solute concentrations.

Introduction

In liquids containing a solute, natural convection driven by both temperature and solute concentration gradients in the liquid phase has a considerable influence on the solidification process in multi-component systems. Temperature gradients may be externally imposed *(i.e.,* by heating/cooling) and are caused internally by the latent heat release or absorption within the mushy zone. During solidification, solute may be incorporated or rejected, therefore inducing local compositional gradients at the solid-liquid interface. This convective flow, driven by both thermal and solutal buoyancy forces, is commonly recognized as double-diffusive natural convection in solidification [1-4]. When growing single crystals from a melt it is desirable that any impurities that originate from the walls of the crucible do not migrate into the mushy region and consequently deposit in the crystal. On the other hand, it is highly desirable to achieve a distribution of dopants in the crystal that is as uniform as possible [5]. Similarly, microsegregation results in the interdendritic spaces when freezing a solute-enriched liquid. Macrosegregation, on the other hand, causes non-uniformity of composition in the cast section on a larger scale [6]. Another example is in the manufacturing of composites and functionally graded materials. We recently demonstrated that control of the distribution of micro-particles and a solute in a thermo-convective flow could be achieved by applying appropriate distributions of magnetic [5, 7] fields acting on the electrically conducting fluid containing the solute [8, 9]. In this work, we will demonstrate the combined use of optimized thermal and magnetic boundary conditions while solidifying thermosolutal flow in a square cavity subjected to variable thermal and magnetic boundary conditions. In this work we will utilize an MHD (magnetohydrodynamics) model [10] and simultaneously optimize thermal and magnetic

boundary conditions in order to reduce concentration gradient induced buoyancy by minimizing vertical gradients of solute concentration in the liquid during solidification.

For the mushy region, the concentrations of the liquid and solid phases, C_l and C_s, are related through the partition coefficient, n, defined as [11]

$$C_s = nC_l \tag{1}$$

where $0 < n < 1$. In order to obtain a more robust model, let us define

$$C = f_s C_s + f_l C_l \qquad D = f_s \rho_s D_s + f_l \rho_l D_l \tag{2.a,b}$$

The subscripts s and l refer to the liquid and solid phases, respectively. Volume fractions g_s and g_l are related to the mass fractions f_s and f_l by [12, 13]

$$\rho\, f_s = \rho_s\, g_s \qquad \rho\, f_l = \rho_l\, g_l \tag{3.a,b}$$

where the local mixture density is defined as

$$\rho = \rho_s\, g_s + \rho_l\, g_l \tag{4}$$

Considering a binary mixture, where the liquidus line in the phase diagram can be represented as a straight line, one can obtain the following equations for the mushy.

$$C_l = \frac{T_m - T}{T_m - T_e} C_e \qquad C_s = \frac{T_m - T}{T_m - T_e} nC_e \tag{5.a,b}$$

Here, T_m is melting temperature, T_e is the eutectic temperature, and C_e is solute concentration at the eutectic temperature. The solid fraction can be modeled by the Lever Rule [11]

$$f_s = \frac{1}{1-n}\left(\frac{T_l - T}{T_m - T}\right) \tag{6}$$

which assumes that the diffusion of the solid is infinite. Mixing in the liquid is primarily by convection and hence it may be quite fast. Therefore, assumption of complete mixing in the liquid is often reasonable. On the other hand, mixing in the solid is by diffusion, which is a very slow process [14]. Therefore, assumption of complete mixing in the solid is not always valid. With the assumption of complete mixing in the liquid and the extreme assumption of no diffusion in the solid, the solid fraction can be described by the Scheil's Model [11]

$$f_s = 1 - \left(\frac{T_m - T}{T_m - T_l}\right)^{\frac{1}{n-1}} \tag{7}$$

In either the Lever Rule or Scheil's equation, one must determine the temperature of solidification and melting of the mixture at a given concentration. Considering the liquidus line as a straight line, one can obtain the following equation by inspection of the binary diagram.

$$T_l = T_m - (T_m - T_e)\frac{C}{C_e} \qquad T_s = MAX\left[T_e, T_m - (T_m - T_e)\frac{C}{nC_e}\right] \tag{8.a,b}$$

Invoking the hypothesis of thermodynamic equilibrium for the temperature implies constant density. Mixture enthalpy per unit mass, h, and mixture thermal conductivity, k, are defined as

$$h = g_s h_s + g_l h_l \qquad k = g_s k_s + g_l k_l \tag{9.a,b}$$

Then, for the case of a binary mixture,

$h < h_{\text{solid}}$

$$T = \frac{h}{C_{Ps}} \tag{10}$$

$h > h_{\text{liquid}}$

$$T = \frac{h + T_s(C_{Pl} - C_{Ps}) - L}{C_{Pl}} \tag{11}$$

$h_{\text{solid}} < h < h_{\text{liquid}}$

$$T = \frac{h + [T_s(C_{Pl} - C_{Ps}) - L](1 - f_s)}{C_{Pl} + f_s(C_{Ps} - C_{Pl})} \tag{12}$$

where the solid mass fraction, f_s, is given by Eqs. (6) or (7), respectively for the Lever Rule and Scheil's Model [11]. Here, L is the latent heat of liquid-solid phase change. Note that if $T < T_{\text{solid}}$, then f_s must be set to unity. If $T > T_{\text{liquid}}$, then f_s must be set to zero. The other thermal properties were approximated as linear functions within the mushy region ($T_{\text{solid}} < T < T_{\text{liquid}}$) and kept constant within each phase. Note that enthalpy is a function of the temperature which is a function of the solid fraction that is itself a function of the temperature. Thus, if $h_{\text{solid}} < h < h_{\text{liquid}}$, we must solve a non-linear system for T. From Eqs. (6), (7) and (12) it follows that

$$T - \frac{h + [T_s(C_{Pl} - C_{Ps}) - L]\left[1 - \frac{1}{1-n}\left(\frac{T_l - T}{T_m - T}\right)\right]}{C_{Pl} + \frac{1}{1-n}\left(\frac{T_l - T}{T_m - T}\right)(C_{Ps} - C_{Pl})} = 0 \tag{13.a}$$

$$T - \frac{h - [T_s(C_{Pl} - C_{Ps}) - L]\left[\left(\frac{T_m - T}{T_m - T_l}\right)^{\frac{1}{n-1}}\right]}{C_{Pl} + \left[1 - \left(\frac{T_m - T}{T_m - T_l}\right)^{\frac{1}{n-1}}\right](C_{Ps} - C_{Pl})} = 0 \tag{13.b}$$

for the Lever Rule and Scheil's Model, respectively. These equations can be solved for T by the secant method. Once T is obtained, and knowing the value of C, the values of the liquid and solid concentrations can be obtained by inspecting the binary diagram. After calculating T and f_s, if the local instantaneous mass fraction of solid is equal to zero, then the local instantaneous concentration of the liquid, C_l, is set to one and the concentration of the solid, C_s, is set to zero. Otherwise, if the local instantaneous solid fraction is equal to one, then the concentration of the liquid, C_l, is set to zero and the concentration of the solid, C_s, is set to one.

General System of Equations

The solidification problem of laminar magneto-hydro-dynamic (MHD) natural convection of an incompressible Newtonian fluid with all physical properties assumed constant has a well-known mathematical model involving a combination of Navier-Stokes equations and Maxwell equations

[10]. The energy source term resulting from viscous dissipation, radiative heat transfer, and Soret and Dufour effects are neglected [15]. Buoyancy effects are approximated by the Oberbeck-Boussinesq hypothesis. Then, the MHD model in this case can be written, for two-dimensional Cartesian coordinate system, as

$$\frac{\partial Q}{\partial t}+\frac{\partial E}{\partial x}+\frac{\partial F}{\partial y}=S \tag{14}$$

$$Q=\lambda\phi \tag{15}$$

$$E=\lambda u\phi^{*}-\Gamma\frac{\partial\phi^{***}}{\partial x} \tag{16}$$

$$F=\lambda v\phi^{**}-\Gamma\frac{\partial\phi^{***}}{\partial y} \tag{17}$$

The values of S, λ, ϕ, ϕ^{*}, ϕ^{**},ϕ^{***} and Γ are given in Table I for the equations of conservation of mass, species, x-momentum, y-momentum, energy, magnetic flux in the x-direction and magnetic flux in the y-direction. Note that we used the Oberbeck-Boussinesq approximation for the variation of the density with temperature and concentration in the y-momentum conservation equation only. Also note that in the energy conservation equation, the term C_PT was replaced by the enthalpy, h, per unit mass. This is useful for problems dealing with phase change where we could use the enthalpy method [12].

For the mushy zone model [6, 12], which is applicable to amorphous materials (waxes and glasses), and the equiaxed zone of metal casting, the solid is assumed to be fully dispersed within the liquid and that velocity vector fields of both solid and liquid phases in the mushy region are the same. The velocity within the solid phase is reduced to a negligible level by explicitly imposing a large difference of viscosity between the solid and liquid phases, such that solid phase viscosity was five orders of magnitude larger than liquid phase viscosity.

Table I. Parameters for the Navier-Stokes and Maxwell equations

Conservation of	λ	ϕ	ϕ^{*}	ϕ^{**}	ϕ^{***}	Γ	**S**
Mass	ρ	1	1	1	1	0	0
Species	ρ	C	C	C	C	D	$\nabla\cdot\left[f_s\rho_s D_s\nabla\left(C_s-C\right)\right]$ $+\nabla\cdot\left[f_l\rho_l D_l\nabla\left(C_l-C\right)\right]$
x-momentum	ρ	u	u	u	u	μ	$-\frac{\partial p}{\partial x}-\frac{B_y}{\mu_m}\left[\frac{\partial B_y}{\partial x}-\frac{\partial B_x}{\partial y}\right]$
y-momentum	ρ	v	v	v	v	μ	$-\frac{\partial p}{\partial y}-\rho g\left[1-\beta\left(T-T_0\right)-\beta_S\left(C-C_0\right)\right]$ $+\frac{B_y}{\mu_m}\left[\frac{\partial B_y}{\partial x}-\frac{\partial B_x}{\partial y}\right]$
Energy	ρ	h	h	h	T	k	$\frac{C_P}{\sigma\mu_m^2}\left[\frac{\partial B_y}{\partial x}-\frac{\partial B_x}{\partial y}\right]^2$
Magnetic x-flux	1	B_x	0	B_x	B_x	$\frac{1}{\mu_m\sigma}$	$\frac{\partial\left(uB_y\right)}{\partial y}$
Magnetic y-flux	1	B_y	B_y	0	B_y	$\frac{1}{\mu_m\sigma}$	$\frac{\partial\left(vB_x\right)}{\partial x}$

Equations in Table I were transformed from the physical Cartesian *(x, y)* coordinates to the computational coordinate system (ξ,η) and solved by the finite volume velocity-pressure coupling SIMPLEC method [16]. The WUDS interpolation scheme [17] was used to obtain the values of u, v, h, B_x and B_y as well as their derivatives at the interfaces of each control volume. The resulting linear system was solved by the GMRES method [18] to accelerate iterative convergence rate.

Validation of the Analysis Code for a Transient Solidification of a Binary Mixture

The MHD analysis code was validated against available analytical and experimental benchmark test cases [7-9, 19]. They involved forced convection in regular and irregular channels, natural convection in regular and irregular cavities, forced convection in the presence of magnetic fields (Pouiseuille-Hartmann Flow), phase change in heat conduction and heat convection problems, natural convection in the presence of magnetic fields, steady-state cooperating thermosolutal convection in enclosures and transient cooperating thermosolutal convection in enclosures. Let us now compare the following mathematical model with the results obtained by Voller *et al.* [12]. They used the SIMPLE method [16] to solve a thermosolutal problem with solidification in a square cavity of size 0.025 m, where all surfaces were insulated, except for the left vertical wall which was suddenly cooled to a temperature below the melting temperature. They used a grid of 30 x 30 cells which, in spite of being very coarse was also used in this work. They did not mention if they used the co-located or staggered grid scheme.

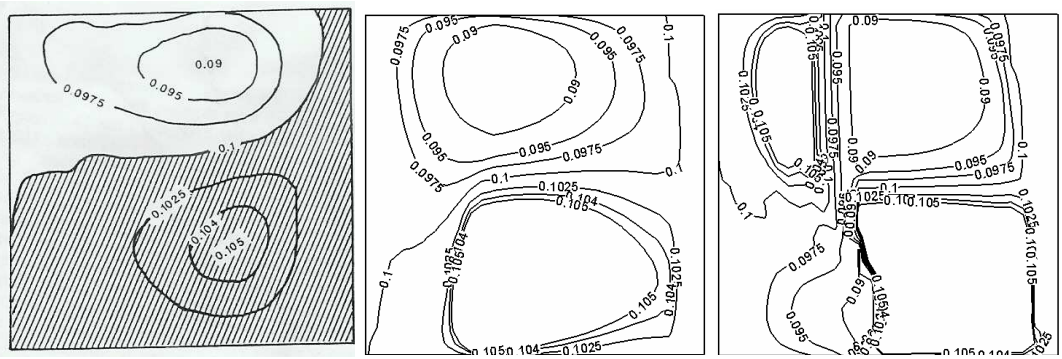

(a) (b) (c)

Figure 1. Comparison between Voller *et al.* [12] (a) and current results for the macro segregation profiles at t = 3000 s, utilizing Voller *et al.* concentration equation with much smaller time step (b) and when using concentration equation from Table I (c).

In the original Voller *et al.* paper, the time step for the numerical integration was taken as one second. In the present results, the time step was taken as 0.001 seconds. Voller *et al*. used a more detailed species conservation equation than given in Table I. Note that this equation, despite being applicable only inside the mushy zone, was used in the entire domain. One can see that the results are very similar for the case when we used Voller *et al.* equation with much smaller integration time step, but are quite different when using equation from Table I.

Multilevel Hybrid Optimizer With a Response Surface

A hybrid optimization is a combination of the deterministic and the evolutionary/stochastic methods, in the sense that it utilizes the advantages of each of these methods. The hybrid optimization method usually employs an evolutionary/stochastic method to locate a region where the global extreme point is located and then automatically switches to a deterministic method to get to the exact point faster. Specifically, it switches automatically among four different methods

of optimization, namely: the Broyden-Fletcher-Goldfarb-Shanno (BFGS) quasi-Newton method, the particle swarm method and the differential evolution method [20].

In order to speed-up the optimization task, the optimization procedure starts with a very coarse grid and then proceeds through a sequence of refined grids. In this paper we also used an interpolation scheme based on the radial basis function method [21, 22]. Thus, after a certain number of objective functions were calculated, all this information was used to obtain a response surface. Such a response surface is then optimized using the same proposed hybrid code so that it fits the calculated values of the objective function as closely as possible. New values of the objective function are then obtained very cheaply by interpolating their values from the response surface. If the BFGS cannot find any better solution, the algorithm uses a radial basis function interpolation scheme to obtain a response surface and then optimizes such response surface using the same hybrid algorithm proposed. When the minimum value of this response surface is found, the algorithm checks if it is also a solution of the original problem. Then, if there is no improvement of the objective function, the entire population is eliminated and a new population is generated around the best value obtained so far. The algorithm returns to the particle swarm method in order to check if there are no changes in this location and the entire procedure repeats itself. After a specified maximum number of iterations is performed (*e.g.,* five) the process stops. Details of certain parts of this hybrid optimizer as well as other optimizers can be found in a recent tutorial [20].

Determining the Unknown Thermal and Magnetic Field Boundary Conditions

The geometry considered is a square cavity, whose height and length are equal to 150 mm. All boundaries were impermeable both to the velocities and to the concentration. The top and bottom walls were kept thermally insulated. The initial thermal condition was set equal to 1685.04 K throughout the container, while the melting temperature was set to T_m = 1685 K. During the optimization process, the temperature of the "hot" right vertical wall was kept constant at 1685.04 K, while the temperature of the "cold" left vertical wall was allowed to vary in the range between 1620 K and 1630 K at each boundary point. Thus, a solidification front starts from the left "cold" wall and a combined buoyancy force due to the thermal and solutal gradients causes the fluid flow. The objective of the optimization was to minimize the natural convection effects by reducing vertical gradient of solute concentration within the liquid zone. The objective function that was minimized was then formulated as

$$F = \sqrt{\frac{1}{\#\text{liquid cells}} \sum_{i=1}^{\#\text{liquid cells}} \left(\frac{\partial C_i}{\partial y_i} \right)^2} \tag{18}$$

The optimization objectives were to be achieved by allowing simultaneous variation of the normal components of the boundary values of the externally imposed magnetic field on the right vertical "uniformly hot" wall and on the bottom thermally insulated wall. In addition, the optimization objective was to be achieved by allowing temperature to vary along the vertical left "cold" wall. The magnetic field and thermal boundary conditions were discretized at six points equally spaced along the x = 0.0 and along y = 0.0 boundaries and interpolated using B-splines for the other points at those boundaries. The magnetic boundary conditions at x = 150 mm and y = 150 mm were then obtained using periodic conditions. Thus the number of parameters to be optimized were equal to 18 (six for the magnetic boundary conditions at x = 0.0, six for the magnetic boundary conditions at y = 0.0 mm and six for the thermal boundary conditions at x = 0.0 mm – "cold wall"). The number of individual distributions of thermal and magnetic boundary conditions in the optimization population necessary for the particle swarm method was set equal to 50, which is approximately 2.7 times greater than the number of parameters to be optimized.

The initial condition for the concentration was set equal to C_0 = 0.1 kg m^{-3}. The eutectic temperature and concentration were set to Te = 1681 K and Ce = 0.8 kg m^{-3}, respectively. The equilibrium partition coefficient was set to n = 0.3 and the final time of the simulation was one hour. The physical properties were taken for molten silicon [9] as

ρ_l = 2550 kg m^{-3}	ρ_s = 2550 kg m^{-3}	k_l = 64 W m^{-1} K^{-1}	k_s = 64 W m^{-1} K^{-1}
C_{Pl} = 1059 J kg^{-1} K^{-1}	C_{Ps} = 1059 J kg^{-1} K^{-1}	μ_l = 0.0032634 kg m^{-1} s^{-1}	μs = 326.34 kg m^{-1} s^{-1}
σ_l = 12.3 x 10^5 1/m Ω	σ_s = 4.3 x 10^4 1/m Ω	β = 1.4 x 10^{-4} K^{-1}	βs = 0.0875
D_l = 6.043 x 10^{-9} kg m^{-1} s^{-1}	D_s = 0 kg m^{-1} s^{-1}	g = 9.81 m s^{-2}	μ_m = 1.2566 x 10^{-5} T m A^{-1}
L=1.8 x 106 J kg^{-1}			

Figure 2 shows the calculated iso-voids, iso-concentrations, and velocity vectors predicted for this test case without any magnetic field applied for four different times: t = 15 min, 30 min, 45 min, and 60 min. One can see the large curvature profile for both the void fraction and the concentration lines. A void fraction equals to one represents a pure solid, while a void fraction equals to zero represents a pure liquid. It is worth to note that the solid phase rejects solute to the liquid phase, as the solidification front propagates upwards, as one can see on the bottom of Fig. 2. For this case, the temperature at the left "cold" wall was set to 1624.96 K.

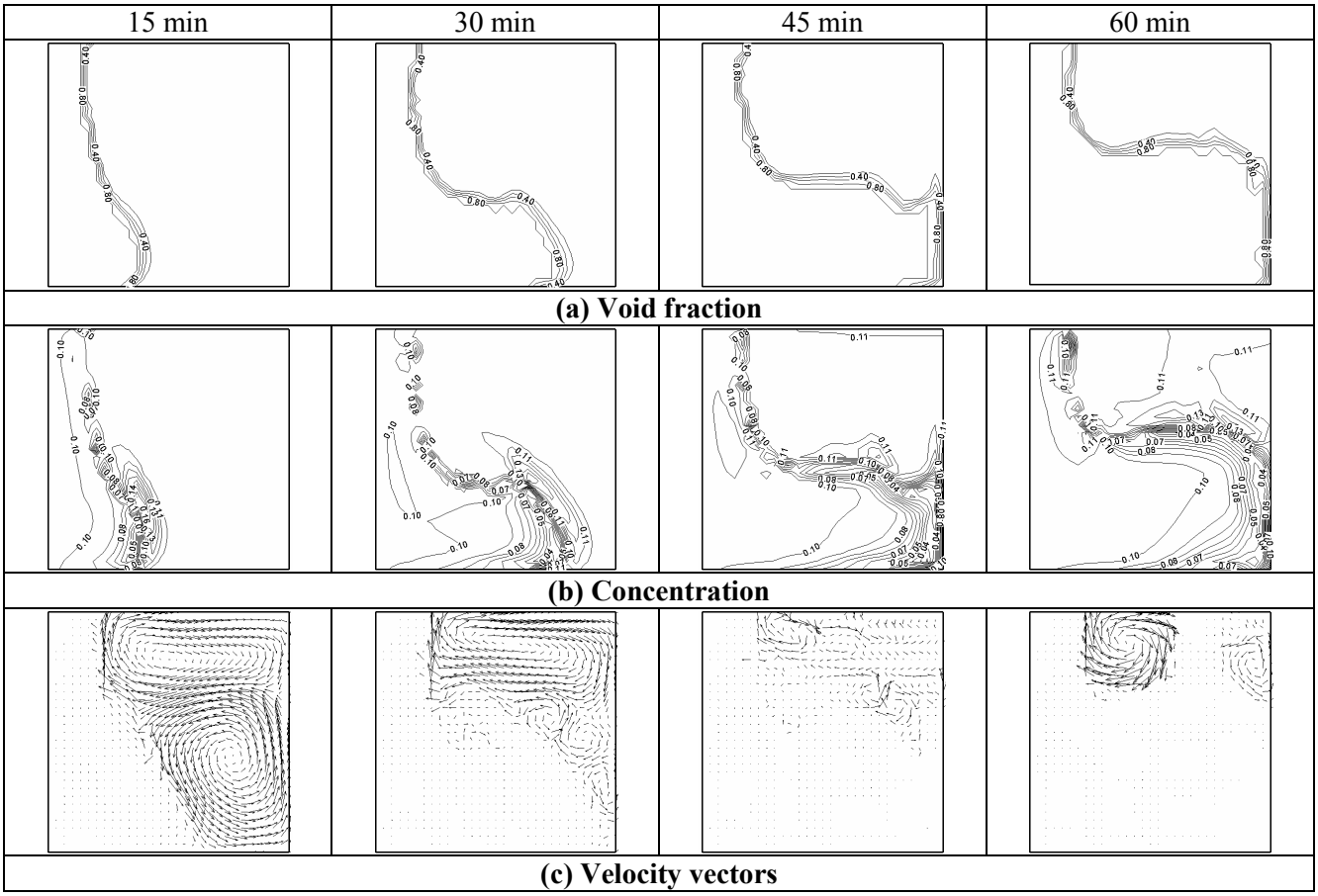

Figure 2. Iso-void (a) and iso-concentration (b) profiles and velocity vectors (c) with no applied magnetic field (**B** = 0) and constant temperature on the vertical left "cold" wall.

Figure 3 shows iso-voids, iso-concentrations, and the velocity vectors resulting from six optimized terms in the B-spline on each boundary for the estimation of the magnetic boundary conditions and thermal boundary conditions on the "cold" wall for four different times. Under the influence of the optimized magnetic field, the iso-concentration profiles are more flat. Using

more design variables (B-spline control points) in the optimization could create even better results where the gradients of concentration in the y-direction would be further reduced.

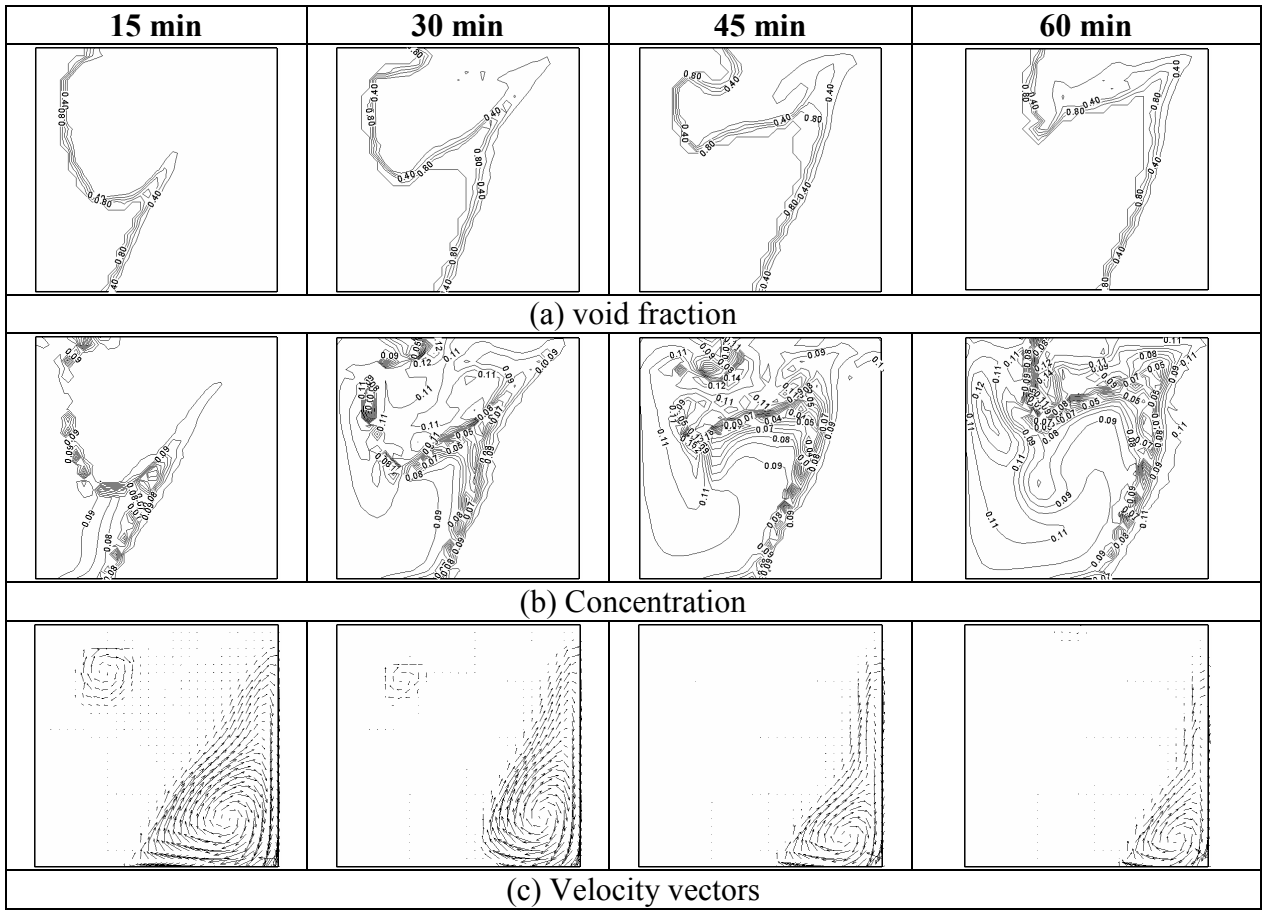

Figure 3. Iso-void (a) and iso-concentration (b) profiles and velocity vectors (c) resulting from magnetic flux **B** optimized at six B-spline points per boundary and temperature optimized at six B-spline points on the left vertical "cold" boundary.

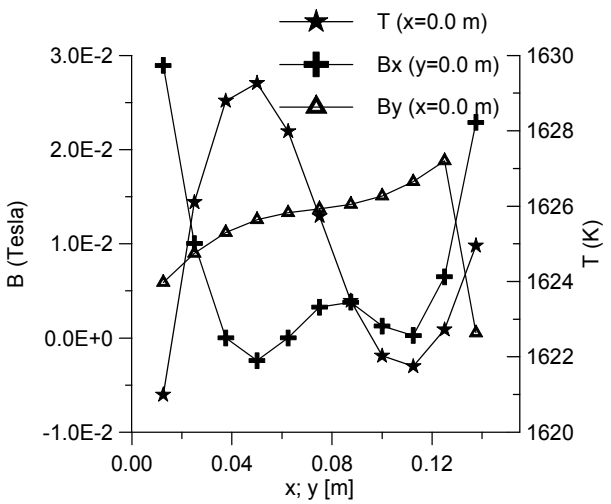

Figure 4. Optimized magnetic and thermal boundary conditions at $x = 0$ and $y = 0$ with the estimation of magnetic flux B and "cold" wall temperature at six points per boundary.

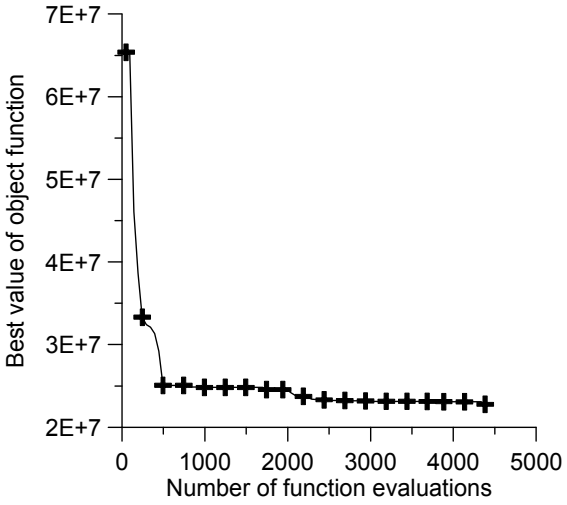

Figure 5. Convergence history of the multilevel hybrid optimization process of thermal and magnetic boundary conditions.

Figure 4 shows the optimized magnetic and thermal boundary conditions for $x = 0$ and $y = 0$. Notice that the strengths of the required magnetic field are very small and could be easily achieved with small permanent magnets. It is quite interesting that the algorithm tries to maintain a larger value of the temperature for the upper half of the container, in such a way that this could minimize the natural convection within the liquid area.

Finally, Fig. 5 shows the convergence history, where the number of function evaluations means the number of times that the solver for the Navier and Maxwell equations is called. For these results we used two grids in the multigrid optimizer. The first grid had 10x10 cells and the final grid had 30x30 cells. The results are presented for the finer grid.

Conclusions

In this paper we presented the results of a transient MHD analysis code that is capable of dealing with thermosolutal problems with and without phase change in enclosures. The code was validated against analytical and numerical (benchmark) results showing good agreement and was applied to test cases involving steady state optimization. The ability to minimize the natural convection effects in problems involving phase change was demonstrated by utilizing an optimized distribution of magnetic and temperature fields along the boundaries of a solidification container. A surface response hybrid optimization algorithm was used.

Due to high computational cost involved in this optimization work, only a coarse grid was used in this work. Although the quantitative results were not fully converged, the qualitative behavior was studied and the methodology was demonstrated. In future works, faster algorithms and a more refined grid should be used. Also, time dependent boundary conditions could be optimized, thus creating an optimal control algorithm for solidification of binary mixtures.

Acknowledgements

This work was partially funded by CNPq (agency for the fostering of science from the State of Brazilian government). The first author is grateful also for the financial support obtained from Florida International University. Both authors are grateful for the partial financial support provided by the AFOSR grant FA9550-06-1-0170 monitored by Dr. Todd E. Combs and by the ARO grant 50486-MS-H monitored by Dr. William M. Mullins.

References

[1] W.D. Bennon and F.P. Incropera, “Numerical simulation of binary solidification in a vertical channel with thermal and solutal mixed convection”, *Int. J. Heat Mass Transfer*, 31 (10), 2147-2160 (1988).

[2] J. Ni and F.P. Incropera, “Extension of the continuum model for transport phenomena occurring during metal alloy solidification-l. The conservation equations”, *J. Heat & Mass Transfer*, 38 (7), 1271-1284 (1995).

[3] R. Sampath and N. Zabaras, “Numerical study of convection in the directional solidification of a binary alloy driven by the combined action of buoyancy, surface tension, and electromagnetic forces”, *J. Comp. Physics*, 168 (2), 384-411 (2001).

[4] J.C. Heinrich and D.R. Poirier, “Convection modeling in directional solidification”, Comptes Rendus Mecanique, 332 (5-6), 429-445 (2004).

[5] S. Motakeff, “Magnetic field elimination of convective interference with segregation during vertical-Bridgman growth of doped semiconductors”, *J. of Crystal Growth*, 104, 833-850 (1990).

[6] A. Ghosh, Segregation in cast products, *Sadhana*, 26, 5-24 (2001).

[7] G.S. Dulikravich, M.J. Colaco, T.J. Martin and S.-S. Lee, "Magnetized fiber orientation and concentration control in solidifying composites", *Journal of Composite Materials*, 37 (15) 1351-1366 (2003).

[8] M.J. Colaço and G.S. Dulikravich, "A multilevel hybrid optimization of magnetohydrodynamic problems in double-diffusive fluid flow", Proceedings of the third meeting of the Study of Matter at Extreme Conditions (SMEC), ed.: Saxena, S., Miami Beach, FL, April 17-21, (2005); also, to appear in *Journal of Physics and Chemistry of Solids*.

[9] M.J. Colaço and G.S. Dulikravich, "Obtaining pre-specified concentration profiles in thermosolutal flows by applying magnetic fields having optimized intensity distribution", Int. Conf. on Computational Methods for Coupled Problems in Science and Engineering, COUPLED PROBLEMS 2005, (eds: M. Papadrakakis, E. Oñate and B. Schrefler), Santorini, Greece (2005).

[10] H.-J. Ko and G.S. Dulikravich, "A fully non-linear model of electro-magneto-hydrodynamics", *International J. of Non-Linear Mechanics*, 35 (4) 709-719 (2000).

[11] M. Rappaz, "Modelling of microstructure formation in solidification processes", *International Materials Review*, 34, 93-123 (1989).

[12] V.R. Voller, A.D. Brent and C. Prakash, "The modeling of heat, mass and solute transport in solidification systems", *Int. J. Heat Mass Transfer*, 32, 1719-1731 (1989).

[13] N. Zabaras and D. Samanta, "A stabilized volume-averaging finite element method for flow in porous media and binary alloy solidification processes", *International Journal for Numerical Methods in Engineering*, 60, 1103-1138 (2004).

[14] A. Ghosh, Segregation in cast products, *Sadhana*, 26, 5-24 (2001).

[15] R. Bennacer and D. Gobin, "Cooperating thermosolutal convection in enclosures – I. Scale analysis and mass transfer", *Int. J. Heat Mass Transfer*, 39, (13), 2671-2681 (1996).

[16] J.P. Van Doormal and G.D. Raithby, "Enhancements of the SIMPLE method for predicting incompressible fluid flow", *Numerical Heat Transfer*, 7, 147-163 (1984)

[17] G.D. Raithby and K.E. Torrance, "Upstream-weighted differencing schemes and their application to elliptic problems involving fluid flow", *Computers & Fluids*, 2, 191-206 (1974).

[18] Y. Saad and M. Schultz, "Conjugate gradient-like algorithms for solving non-symmetric linear systems," *Mathematics of Computation*, 44, 170 (1985).

[19] M.J. Colaço, G.S. Dulikravich and T.J. Martin, **"**Control of Unsteady Solidification via Optimized Magnetic Fields", Materials and Manufacturing Processes, 20 (3) 435-458 (2005).

[20] M.J. Colaço, G.S. Dulikravich, H.R.B. Orlande and T.J. Martin, "Hybrid Optimization with Automatic Switching Among Optimization Algorithms", in: *Handbooks on Theory and Engineering Applications of Computational Methods: Evolutionary Algorithms and its Applications*, eds. Onate, Annicchiarico, Periaux, Barcelona, Spain, CIMNE (2005).

[21] E.J. Kansa, "Multiquadrics – A Scattered Data Approximation Scheme with Applications to Computational Fluid Dynamics – II: Solutions to Parabolic, Hyperbolic and Elliptic Partial Differential Equations", *Comput. Math. Applic.,* 19, 149-161 (1990).

[22] V.M.A. Leitão, "A Mesheless Method for Kirchhoff Plate Bending Problems", *International Journal of Numerical Methods in Engineering*, 52, 1107-1130 (2001).